THE JOURNAL OF PHYSICAL CHEMISTRY A

pubs.acs.org/JPCA Article

Be–Be Bond in Action: Lessons from the Beryllium–Ammonia Complexes $[Be(NH_3)_{0-4}]_2^{0,2+}$

Published as part of The Journal of Physical Chemistry virtual special issue "Alexander Boldyrev Festschrift".

Isuru R. Ariyarathna and Evangelos Miliordos*

Cite This: *J. Phys. Chem. A* 2020, 124, 9783–9792 Read Online

ACCESS | Metrics & More | Article Recommendations | Supporting Information

ABSTRACT: High-level electronic structure calculations are performed to elucidate the Be–Be chemical bond in the $(NH_3)_nBe–Be(NH_3)_n$ species for n = 0–4. We show that the Be_2 bond is explained as a resonance between two Lewis structures, where one beryllium atom donates an electron pair to the second one, and vice versa. The presence of ammonia ligands enhances the stability of this bond considerably. The ∼2.5 kcal/mol binding energy of Be_2 becomes ∼30 kcal/mol for $[Be(NH_3)_{1-3}]_2$ because of their more polarizable electron pairs. The larger $Be(NH_3)_4$ complex has been classified as a solvated electron precursor in the past and has an electron pair in the periphery of a $Be(NH_3)_4^{2+}$ core occupying a diffuse s-type orbital. The analogy of $Be(NH_3)_4$ to Be reflects into the electronic structure of their dimers. The two systems have identical bonding patterns and low-lying electronic states. The ground state binding energy of $[Be(NH_3)_4]_2$ is 3 times larger than Be_2, and its excitation energies are considerably lower by a factor of 3. We also studied the dimers of the cationic $Be(NH_3)_n^+$ species, and we found that the Coulombic repulsion is counterbalanced by the formation of a single covalent bond in the cases of n = 1, 2 forming stable dicationic $[(NH_3)_nBe–Be(NH_3)_n]^{2+}$ systems, unlike Be_2^{2+}. We believe that our numerical results will allow the identification and characterization of these exotic species and their solid state (beryllium liquid metals) analogues in future experiments.

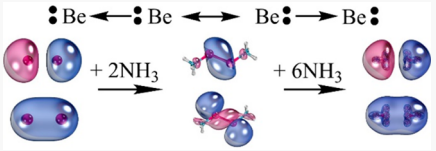

I. INTRODUCTION

The interaction energy between two identical noble gas atoms is as small as 7.26 cm^{-1} (He–He interaction).[1] This weak electrostatic attraction increases with the size (or more accurately the polarizability) of the atom to 29.40 and 99.2 cm^{-1} for the Ne and Ar dimers.[2,3] Chemical bonding is observed only between their excited states, where unpaired electrons are present. See for example the potential energy curves of ref 4 and the spectroscopic study of ref 5 regarding He_2. The ground state of Be is a $1s^22s^2$ closed-shell singlet state, and its dimer is expected to form a weakly bound system. However, the experimental Be_2 interaction energy of 929.7 cm^{-1} (30 times larger than its second-row noble gas analogue, Ne_2) and its 2.45 Å equilibrium distance[6] (as opposed to the 2.98 Å equilibrium distance of the smaller He_2)[1,7] pose questions about the nature of the Be–Be bond.

The bonding in Be_2 has attracted the interest of several quantum chemical studies (see refs 6 and 8–10 and references therein). The recent high-level electronic structure calculations by Kalemos point to a complex wave function of rather multireference nature with a 79% weight for the most dominant configuration.[8] Kalemos further claimed that the global minimum of Be_2 actually originates from the double bond of two $^3P(1s^22s^12p^1)$ excited beryllium atoms. The complex nature of the Be_2 bond reflects to the difficulty of calculating its dissociation energy accurately. For example, Patkowski et al. found that the "golden standard" all-electron CCSD(T) level of theory gives a value of 715 ± 6 cm^{-1} at the complete basis set limit (only 77% of the experimental value).[10] These authors found that the $1s^2$ electron correlation for Be is important and contributes to this number by 85 cm^{-1}. The addition of higher electron "excitations" through full configuration interaction (FCI) calculations were found indispensable to obtain a more accurate value of 942 cm^{-1}.[10] Kalemos, on the other hand, demonstrated that the problem is the "pathologically inappropriate" description of the zero order level wave function (Hartree–Fock–Slater determinant in the case of CCSD(T)) and emphasized the necessity of high-angular momentum basis functions.[8]

The addition of ligands to Be_2 induces the promotion of the beryllium centers to *in situ* excited electronic states facilitating the formation of stronger Be–Be bonds. See, for example, the double bond of around 10 kcal/mol in $(CO)_2BeBe(CO)_2$,[11] the HBeBeH,[12,13] and FBeBeF[14] molecules with 85 and 77 kcal/mol dissociation energies or the exotic Be–Li clusters.[15] In the HBeBeH case, the Be–H bond formation places Be to its first excited state ^3P $(1s^22s^12p^1)$, 21980 cm^{-1} above its $^1S(1s^2s^2)$ ground state,[16] creating a ground ·BeH $(^2\Sigma^+)$ state.[8]

Received: August 31, 2020
Revised: October 9, 2020
Published: October 15, 2020

The two electrons localized at the two beryllium ends form a covalent Be−Be bond. A similar scheme can be inferred for FBeBeF based on its molecular orbitals.[14] Beryllium is in its ^{3}P state as well in BeCO, which is however metastable dissociating to Be(^{1}S; $1s^2 2s^2$) + CO. On the other hand, $Be(CO)_2$ is stable with respect to Be + 2CO, and the beryllium center is in an even higher *in situ* electronic state, 2^3P ($1s^2 2p^2$) at 59696 cm^{-1}.[17] The stabilization of 2^3P is due to the "simultaneous" OC → Be ← CO dative bonds formation and π-back-donation of the two $2p_\pi$ electrons of Be to π^*-(CO).[17,18] Finally, high electron affinity ligands, such as O_2 or NO, oxidize beryllium to Be^+ or Be^{2+}; see for example $Be(O_2)_{1-2}$ and Be(NO) compounds.[17,19]

Ammonia is found to interact in a completely different manner with Be. Ammonia is a strong σ-donor, but unlike CO it cannot ease π-back-donation. For $Be(NH_3)_3$, we recently found that ammonia instead of inducing electronic excitation of the beryllium center, its lone electrons "displace" partly the beryllium valence electrons to the periphery of the molecular skeleton.[20] The attachment of a fourth ammonia creates a pure $Be^{2+}(NH_3)_4$ center with two peripheral electrons occupying hydrogen-like orbitals.[21] Such systems are referred to as solvated electron precursors, or SEPs.[21−26] The unusual chemistry of ammonia has been attributed to the strong metal−ammonia bonds and the ability of ammonia to solvate electrons.[22] In the case of water, such complexes (called SEPs) are less stable, and the diffuse electrons reduce the water hydrogens ("protons"), releasing easily H_2.[22] The second-row analogue of ammonia, PH_3, acts like CO promoting beryllium to its 2^3P state.[20]

A natural question is how the Be−Be bonding changes with the number of ammonia "ligands" present in the $(NH_3)_n$BeBe-$(NH_3)_n$ (n = 1−3) systems. In addition to the dimers of the neutral beryllium−ammonia complexes, we studied the dimers of the cationic $Be(NH_3)_{n=1-3}^+$ systems, which formed stable dicationic systems, unlike the metastable (by 54.1 kcal/mol) Be_2^{2+}.[14]

Lithium and sodium form the stable (experimentally observed) $Li(NH_3)_4$ and $Na(NH_3)_4$ SEPs, where one electron orbits around $Li(NH_3)_4^+$ and $Na(NH_3)_4^+$.[25] We showed that these H-mimicking molecules can bind together with a single covalent bond of highly diffuse nature exactly like Li_2 or Na_2 is formed by two Li or Na atoms.[25] Furthermore, saturation of ammonia solutions with metal atoms, such as Li, creates polymers of SEPs, known as liquid metals.[27,28] Our present goal is to extend our studies to the Be_2 analogue and investigate the formation of $[Be(NH_3)_4]_2$ and by extension the existence of beryllium liquid metals. Will it act as Be_2 or as He_2? What is the effect of the diffuse nature of the outer electrons and the electronic structure of the $Be(NH_3)_4$ monomer?

In section II we describe the computational details, section III.1 is devoted to $Be(NH_3)$, the $Be(NH_3)_{2-4}$ are discussed in section III.2, their dimers are studied in section III.3, and section III.4 deals with both the monomeric and dimeric cationic systems.

II. METHODS

Optimal structures for all of the $Be(NH_3)_{n=1-3}^{0/+}$ species are obtained at the coupled cluster CCSD(T) level of theory[29] using the triple-ζ quality correlation-consistent aug-cc-pVTZ basis set.[30,31] Harmonic vibrational frequencies were also calculated to confirm the stability of the located minima. For the construction of the potential energy profiles (PEPs) as a function of the Be−N distance for the ground and excited electronic states, we employed the internally contracted multireference configuration interaction (MRCI).[32−34] The N−H bond lengths and Be−N−H bond angles were kept constant and equal to their ground state equilibrium values at all Be−N distances. The cc-pVTZ set is used for the MRCI calculations. Considering that excitations out of the NH_3 electrons are high in energy, the starting CASSCF active space consists of the one/two "beryllium" valence electrons and four active orbitals. These correspond to the 2s and 2p orbitals of Be at long Be−N interatomic distances. All valence electrons are correlated at the MRCI level. For $Be(NH_3)$ and $Be(NH_3)_2$ we optimized the geometries of the excited electronic states at MRCI, but we kept the C_{3v} and C_{2v} symmetry of the ground state. The single-point energy calculations considering the Davidson correction (MRCI +Q)[35] were also performed to account for higher order electron correlation effects using the MRCI geometries.

A similar methodology was used for the $Be(NH_3)_n^{0/+}$ dimers. Because of technical limitations, the optimizations and frequency calculations were performed at CCSD(T)/cc-pVTZ for $[Be(NH_3)_{1,2}]_2^{0/2+}$, at MP2/aug-cc-pVTZ for $[Be(NH_3)_3]_2^{0/2+}$, and at MP2/cc-pVTZ(Be,N) aug-cc-pVTZ(H) for $[Be(NH_3)_4]_2$. For $[Be(NH_3)]_2^{0/2+}$ and $[Be(NH_3)_2]_2^{2+}$, PEPs are constructed with respect to the Be−Be distance at the MRCI level of theory. The equilibrium geometries are used for the construction of the PEPs varying only the Be−Be distance. The active space of $[Be(NH_3)_{1-2}]_2^{0/2+}$ consists of two or four electrons in eight orbitals. For $[Be(NH_3)_4]_2$, the geometry is optimized at every Be−Be distance at the density functional theory DFT/B3LYP level of theory, and CASPT2 calculations followed for the ground excited electronic states. The active space was four electrons into 18 orbitals. These 18 orbitals correspond to the outer 1s, 1p, and 1d superatomic orbitals of the monomers.[21] For the dimers we used the cc-pVDZ basis set for Be and N and the d-aug-cc-pVDZ set for H centers. In every case all valence electrons are correlated at the post-CASSCF level of theory except for the $[Be(NH_3)_4]_2$, where excitations from the CASSCF active orbitals to the virtual space are allowed.

Providing very accurate interaction/binding energies is beyond the scope of this work since FCI calculations may be necessary. We rather aim at the disclosure of the interesting electronic structure features of these systems. Therefore, we compare binding energies of all (small and large) systems at the CCSD(T)/aug-cc-pVTZ and MP2/aug-cc-pVTZ levels (see below for more details about each system).

Finally, we calculated dipole polarizabilities α_{zz} for the $Be(NH_3)_{n=0-4}$ systems, where z is their principal axis of symmetry. To this end, electric fields of f = 0.001 au intensity are applied along the z-axis with both positive and negative polarity. The α_{zz} value is estimated as the second derivative of the energy with respect to the applied field intensity $\partial^2 E/\partial f^2 \approx [E[+f] + E[-f] - 2E[0]]/f^2$, where $E[\pm f]$ and $E[0]$ are the CCSD(T)/aug-cc-pVTZ or MP2/aug-cc-pVTZ energies with the two opposite polarities and zero electric field.

All DFT and MP2 calculations are performed with Gaussian16,[36] and all MRCI, CASPT2, and CCSD(T) calculations are performed with MOLPRO.[37]

https://dx.doi.org/10.1021/acs.jpca.0c07939
J. Phys. Chem. A 2020, 124, 9783−9792

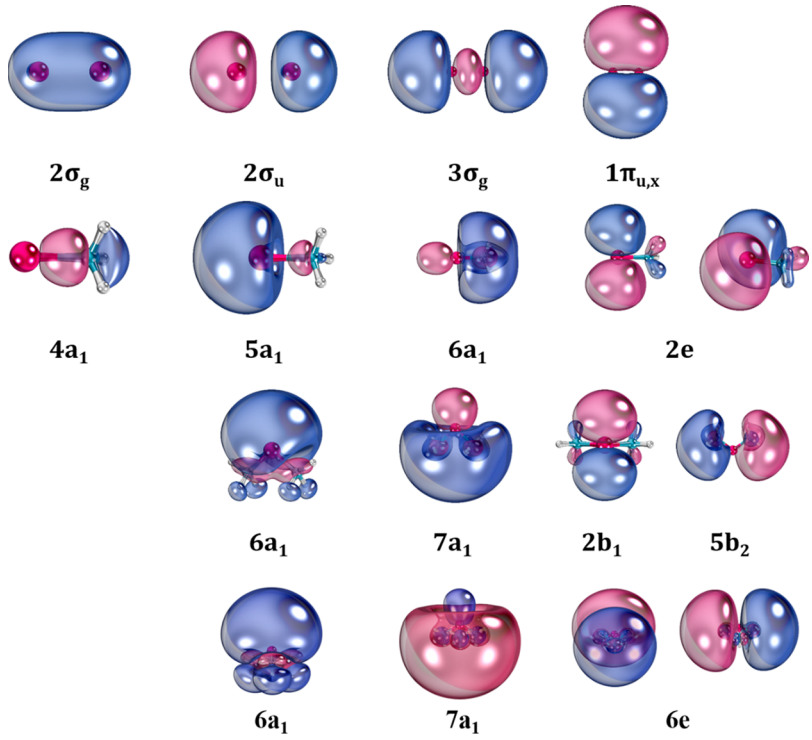

Figure 1. Selected molecular orbitals of Be_2 (first row), $Be(NH_3)$ (second row), $Be(NH_3)_2$ (third row), and $Be(NH_3)_3$ (fourth row).

III. RESULTS AND DISCUSSION

III.1. $Be(NH_3)$ and Be_2. The interaction between the ground closed-shell Be and NH_3 moieties is expected rather repulsive with a shallow potential well at long Be−N distances, as happens for $Be(^1S)$ + $CO(X^1\Sigma^+)$.[17] Indeed, the lowest energy Be−NH_3 CCSD(T)/aug-cc-pVTZ potential energy curve reveals a plateau in the 3 Å region as a result of this interaction. However, the PEC at ∼2.8 Å plunges into a potential well of 1802 cm^{-1} or 5.15 kcal/mol depth with respect to the Be + NH_3 fragments at a Be−N distance of 1.79 Å (see Figure S1 of the Supporting Information). This distance is substantially shorter than that of Be_2 (2.45 Å), and the binding energy is about 4 times larger than that of Be_2 at the same level of theory (472 cm^{-1}), suggesting a weak but present chemical bond. The Be−N harmonic vibrational frequency is ω_e = 456 cm^{-1}, giving an estimate of the zero point vibrational energy of around 228 cm^{-1} and placing the ground vibrational level well below the dissociation limit.

The molecular orbitals of Figure 1 indicate clearly that the electron pair of ammonia "pushes" the electron pair of Be at the "back" of it, making way for the formation of a dative bond from H_3N: to an effective Be^{2+} center. The shielding of the displaced beryllium electrons is still quite efficient to prevent a strong Be−NH_3 bond.

This observation raises the question of whether the bond formation in Be_2 is of similar nature: the electrons of the first beryllium atom "push" the electron pair of the second, and vice versa. The two resonance structures are indistinguishable. In the higher symmetry case of Be_2, the analogous $4a_1$ and $5a_1$ orbitals ($4a_1 \sim 2s_{Be,right}$, $5a_1 \sim 2s_{Be,left}$; see Figure 1) are combined to make orbitals $2\sigma_g$ and $2\sigma_u$ of Be_2 (see Figure 1), which are doubly occupied in the main ($2\sigma_g^2 2\sigma_u^2$; 79%) electronic configuration of Be_2 as happens for $Be(NH_3)$. The second most important electronic configuration ($2\sigma_g^2 3\sigma_g^2$; 7%) of Be_2 involves orbital $3\sigma_g$ (see Figure 1), which is better assigned to a $2p_z$−$2p_z$ covalent bond, in addition to the 2s−2s σ-bonding orbital ($2\sigma_g$ orbital of Figure 1). The latter configuration points to a contribution of a double bond between two Be(^3P; $1s^2 2s^1 2p_z^1$) atoms and has been suggested as the main binding mechanism by Kalemos in the past.[8] Presently, we provide an alternative view of the Be_2 bond depicted in terms of Lewis structures in Scheme 1, which combines these two contributions. The coefficient of the second configuration is even smaller (−0.11 or 1.2%) for $Be(NH_3)$.

Scheme 1. Lewis Structures for the Be−Be Bonding in Be_2

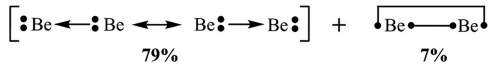

A natural question is why beryllium is special. We believe that beryllium can act as a base and acid at the same time, as opposed to noble gases. Its metallic nature renders it a relatively good base,[20] and its lower excitation energies make it more polarizable and thus eager to displace its electrons in favor of an electron pair of an "attacking" base. Specifically, the polarizability of Be (5.60 $Å^3$) is at least 3 times larger than that of He (0.205 $Å^3$), Ne (0.394 $Å^3$), and Ar (1.64 $Å^3$).[38] Because excitation energies and polarizability are connected (via perturbation theory), an equivalent statement is that given by the authors of ref 9, who assign the difference between Be and He or Ne to the low 2s−2p gap of Be. The proposed chemical bond of Scheme 1 falls under the general category of charge-shift bonds reported recently in the literature.[39]

We turn our discussion to the excited states of $Be(NH_3)$. Complete PEPs for the first five adiabatic channels are plotted in Figure 2, and optimal Be−N distances and excitation energies are listed in Table 1 along with their dominant electronic configurations; the molecular orbitals associated with them are shown in Figure 1. It should be noted that

https://dx.doi.org/10.1021/acs.jpca.0c07939
J. Phys. Chem. A 2020, 124, 9783−9792

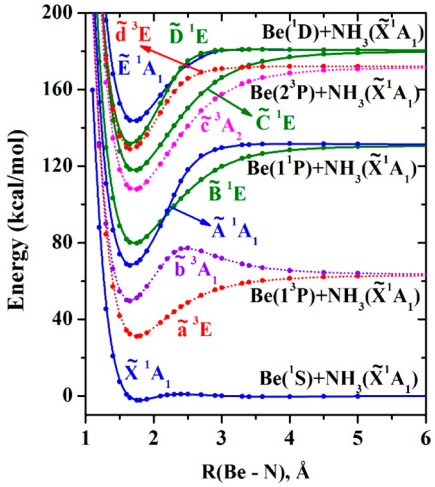

Figure 2. MRCI PEPs of $Be(NH_3)$ as a function of the Be−N distance. All other bond lengths and angles are kept fixed to their optimal values of the ground state global minimum.

Table 1. Excitation Energy ΔE (cm^{-1}), Be−N Bond Length r_{BeN} (Å), and Dominant Electronic Configurations for the Lowest Electronic States of $BeNH_3$

				electronic configuration[a]				
state	method	ΔE	r_{BeN}	coeff	$5a_1$	$6a_1$	$2e_x$	$2e_y$
$\tilde{X}^1A_1$	MRCI	0	1.786	0.95	2	0	0	0
	MRCI+Q	0						
	CCSD(T)	0	1.798					
$\tilde{a}^3E$	MRCI	11571	1.750	1.00	α	0	0	α
	MRCI+Q	12140						
	CCSD(T)	12223	1.755					
$\tilde{b}^3A_1$	MRCI	21781	1.634	1.00	α	α	0	0
	MRCI+Q	21578						
	CCSD(T)	21284	1.641					
$\tilde{A}^1A_1$	MRCI	29145	1.721	0.71	α	β	0	0
	MRCI+Q	27697		−0.71	β	α	0	0
$\tilde{B}^1E$	MRCI	29361	1.720	0.71	α	0	0	β
	MRCI+Q	27790		−0.71	β	0	0	α
$\tilde{c}^3A_2$	MRCI	38595	1.718	1.00	0	0	α	α
	MRCI+Q	38748						
	CCSD(T)	38788	1.722					
$\tilde{C}^1E$	MRCI	42665	1.716	0.71	0	0	α	β
	MRCI+Q	41707		−0.71	0	0	β	α
$\tilde{d}^3E$	MRCI	50026	1.654	1.00	0	α	0	α
	MRCI+Q	49350						
$\tilde{D}^1E$	MRCI	51803	1.643	0.71	0	α	0	β
	MRCI+Q	50160		−0.71	0	β	0	α
$\tilde{E}^1A_1$	MRCI	52103	1.708	0.66	0	0	2	0
	MRCI+Q	56917		0.67	0	0	0	2

[a]Coeff is the coefficient of each determinant, and α, β occupations correspond to spin-up or spin-down electrons. Contours of the relative orbitals are plotted in Figure 1.

harmonic vibrational frequencies were calculated only for the ground state ensuring that the structure is a stable minimum. For the excited states, geometry distortions from the imposed C_{3v} geometry may apply. In addition, the MRCI PEP of the ground state differs from that of CCSD(T) (compare Figure 1 and Figure S1). MRCI predicts a small barrier between the long-range interaction and the binding minimum.

The $2s_{Be}$ orbital composes practically the $5a_1$ orbital, while the 2p orbitals of Be split to the $6a_1$ and 2e orbitals. The latter ones are nearly the $2p_x$ and $2p_y$ orbitals (z being the Be−N axis), while $6a_1$ is a $2p_z$-like orbital diffused toward the N−H terminal bonds. The two valence electrons in the ground $\tilde{X}^1A_1$ state remain in the $\sim 2s_{Be}$ ($5a_1$) orbital. The first four excited states include excitation of one $5a_1$ electron to either $6a_1$ ($\tilde{b}^3A_1$ and $\tilde{A}^1A_1$) or 2e ($\tilde{a}^3E$ and $\tilde{B}^1E$). These states lie between 12000 and 28000 cm^{-1} at MRCI+Q. The same pattern is observed for the lowest lying states of BeCO, except for the ground state PEC, which is purely repulsive.[17] The next batch of states between 38000 and 57000 cm^{-1} involve the promotion of both $5a_1$ electrons to a $6a_1{}^12e^1$ ($\tilde{d}^3E$ and $\tilde{D}^1E$) or $2e^2$ ($\tilde{c}^3A_2$, $\tilde{C}^1E$, and $\tilde{E}^1A_1$) configuration. The bond length in all excited states is shorter than this of the ground state (1.79 Å at MRCI) with the smallest one belonging to $\tilde{b}^3A_1$ (1.63 Å at MRCI), and they are well bound with respect to their adiabatic fragments.

III.2. $Be(NH_3)_2$, $Be(NH_3)_3$, and $Be(NH_3)_4$. The PECs, selected molecular orbitals, and numerical data for the ground and excited states of $Be(NH_3)_2$ and $Be(NH_3)_3$ are provided in Figures 1 and 3 as well as Tables 2 and 3. PEPs for $Be(NH_3)_3$

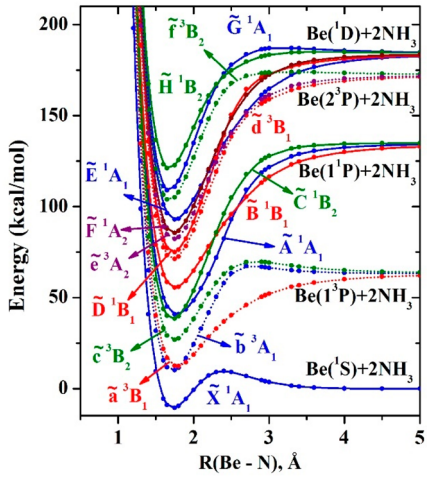

Figure 3. MRCI PEPs of $Be(NH_3)_2$ as a function of the two equal Be−N distances. All other bond lengths and angles are kept fixed to their optimal values of the ground state global minimum.

are given in the Supporting Information (Figure S3) of our previous work.[20] The ground state for both systems retains the $\sim 2s_{Be}{}^2$ configuration, and their PECs are characterized by an "activation barrier" when ammonias approach Be. Interestingly enough, the Be−NH_3 bonds become stronger as more ammonia molecules attach to beryllium. Specifically, the CCSD(T)/aug-cc-pVTZ binding energy per Be−NH_3 bond is 5.2, 8.3, and 12.8 kcal/mol calculated as $[E[Be] + nE[NH_3] - E[Be(NH_3)_n]]/n$, where $E[X]$ is the equilibrium energy of molecule X. It seems that the concerted displacement of the beryllium valence electrons by more ammonias exposes further the Be nuclear charge. The larger effective charge on the beryllium center enhances the stability of the Be−NH_3 bonds.

The excited states of $Be(NH_3)_{2,3}$ follow the same pattern as in $Be(NH_3)$. The promotion of a $6a_1$ ($\sim 2s_{Be}$) electron to one of the $\sim 2p_{Be}$ orbitals provide the lowest energy states. The $7a_1$ orbital is along the principal axis of symmetry in each case ($\sim 2p_{z,Be}$). The remaining two 2p orbitals are degenerate only for $Be(NH_3)_3$ since the C_{2v} symmetry of $Be(NH_3)_2$ lifts their degeneracy ($2b_1$ and $5b_2$ orbitals). The two unpaired electrons

https://dx.doi.org/10.1021/acs.jpca.0c07939
J. Phys. Chem. A 2020, 124, 9783−9792

Table 2. Excitation Energy ΔE (cm^{-1}), Be−N Bond Length r_{BeN} (Å), N−Be−N Angles θ_{NBeN} (deg), and Dominant Electronic Configurations for the Lowest Electronic States of $Be(NH_3)_2$

					electronic configuration[a]				
state	method	ΔE	r_{BeN}	θ_{NBeN}	coeff	$6a_1$	$7a_1$	$2b_1$	$5b_2$
$\tilde{X}^1A_1$	MRCI	0	1.730	101.7	0.95	2	0	0	0
	MRCI+Q	0							
	CCSD(T)	0	1.747	100.3					
$\tilde{a}^3B_1$	MRCI	5933	1.774	110.8	1.00	α	0	α	0
	MRCI+Q	6502							
$\tilde{b}^3A_1$	MRCI	10270	1.694	115.2	1.00	α	α	0	0
	MRCI+Q	10791							
	CCSD(T)	10858	1.703	111.6					
$\tilde{c}^3B_2$	MRCI	16396	1.724	109.2	1.00	α	0	0	α
	MRCI+Q	16661							
$\tilde{A}^1A_1$	MRCI	20281	1.754	112.1	0.65	α	β	0	0
	MRCI+Q	19804			−0.65	β	α	0	0
$\tilde{B}^1B_1$	MRCI	21323	1.757	118.8	0.71	α	0	β	0
	MRCI+Q	20169			−0.71	β	0	α	0
$\tilde{d}^3B_1$	MRCI	21416	1.732	180.0	1.00	0	α	α	0
	MRCI+Q	21579							
$\tilde{C}^1B_2$	MRCI	24796	1.692	116.9	0.71	α	0	0	β
	MRCI+Q	23610			−0.71	β	0	0	α
$\tilde{D}^1B_1$	MRCI	25807	1.687	172.6	0.71	0	α	β	0
	MRCI+Q	24098			−0.71	0	β	α	0
$\tilde{E}^1A_1$	MRCI	27904	1.652	177.9	0.93	0	0	2	0
	MRCI+Q	26479							
$\tilde{e}^3A_2$	MRCI	31746	1.664	177.9	1.00	0	0	α	α
	MRCI+Q	31593							
$\tilde{f}^3B_2$	MRCI	31755	1.664	180.0	1.00	0	α	0	α
	MRCI+Q	31596							
$\tilde{F}^1A_2$	MRCI	32951	1.661	180.0	0.71	0	0	α	β
	MRCI+Q	32371			−0.71	0	0	β	α
$\tilde{G}^1A_1$	MRCI	35415	1.692	180.0	0.60	0	0	0	2
	MRCI+Q	33384			−0.77	0	2	0	0
$\tilde{H}^1B_2$	MRCI	35264	1.664	180.0	0.71	0	α	0	b
	MRCI+Q	33588			−0.71	0	β	0	α

[a]Coeff is the coefficient of each determinant, and α, β occupations correspond to spin-up or spin-down electrons. Contours of the relative orbitals are plotted in Figure 1.

can couple into a singlet or triplet spin multiplicity, making the lowest lying electronic states (see Tables 2 and 3). The promotion of the second $6a_1$ electron to either $7a_1$ or one of the two (quasi-)degenerate $2p_{Be}$ orbitals generates the rest of the studied states.

The range of MRCI+Q excitation energies for the same 15 (counting degenerate states twice) states is 0−56917, 0−33588, and 0−40000 cm^{-1} for one, two, and three ammonia ligands. It is noteworthy that the triplet state with one electron in $\sim 2s_{Be}$ and one in $\sim 2p_{z,Be}$ orbitals is stabilized with the number of ammonias. It is the third excited state at 21578 cm^{-1} for $Be(NH_3)$, it becomes the second excited state at 10791 cm^{-1} for $Be(NH_3)_2$, and ends up the first excited state at 7830 cm^{-1} for $Be(NH_3)_3$. A possible reason is that the $\sim 2p_{z,Be}$ orbital actually diffuses more and more toward the ammonias' terminal, enabling a stronger "solvation" of the occupying electron by more N−H bonds. It should also be mentioned that the *in situ* electronic structure of beryllium within the $Be(NH_3)_{1-3}$ molecule retains the energy order of the isolated beryllium atom. Specifically, $Be(^1S;\ 1s^22s^2)$ corresponds to the ground $6a_1^2$ state, $Be(1^3P$ and $^1P;\ 1s^22s^12p^1)$ relate to the lowest lying states of the complexes, and $Be(2^3P$ and $^1D;\ 1s^22p^2)$ pertain to their higher energy states (see Figures 2 and 3 as well as Figure S3 of ref 20).

The addition of a fourth ammonia leads to $Be(NH_3)_4$, where four ammonia ligands are attached to a Be^{2+} center and the two valence electrons orbit in the periphery of this complex. This last addition turns out to be more exothermic than the other three with a $Be(NH_3)_3 + NH_3$ binding energy of 28 kcal/mol,[21] which gives an average Be−NH_3 bond of 16.6 kcal/mol. Again, the bond energy increases compared to the smaller complexes. The beryllium valence electrons become now electrons of the molecule occupying one of the "super-atomic" orbitals that arise (1s, 1p, 1d, 2s). The type of the three lower electronic states mimic those of Be: $1s^2$ vs $2s_{Be}^2$ (ground state), triplet $1s^11p^1$ vs triplet $2s_{Be}^12p_{Be}^1$ (first excited state), and singlet $1s^11p^1$ vs singlet $2s_{Be}^12p_{Be}^1$ (second excited state). The excitation energies of $Be(NH_3)_4$ are much smaller though: 0.81 vs 2.725 eV and 1.62 vs 5.28 eV.[16,21] How this energy lowering affects the binding of two $Be(NH_3)_4$ moieties compared to Be_2? Do the "intermediates" $Be(NH_3)_{n=1-3}$ moieties bind and how strongly?

III.3. $Be(NH_3)_{n=1-4}$ Dimers. The discussion of section III.4 shows that the addition of ammonia ligands to beryllium retains its $1s^22s^2$ *in situ* electronic state as opposed to other

https://dx.doi.org/10.1021/acs.jpca.0c07939
J. Phys. Chem. A 2020, 124, 9783−9792

Table 3. Vertical Excitation Energy ΔE (cm^{-1}) and Dominant Electronic Configurations for the Lowest Electronic States of $Be(NH_3)_3$

			electronic configuration[a]				
state	method	ΔE	coeff	$6a_1$	$7a_1$	$6e_x$	$6e_y$
$\tilde{X}^1A_1$	MRCI	0	0.95	2	0	0	0
	MRCI+Q	0					
$\tilde{a}^3A_1$	MRCI	7441	1.00	α	α	0	0
	MRCI+Q	7830					
$\tilde{b}^3E$	MRCI	12338	0.96	α	0	α	0
	MRCI+Q	12704					
$\tilde{A}^1A_1$	MRCI	21638	0.71	α	β	0	0
	MRCI+Q	20541	−0.71	β	α	0	0
$\tilde{B}^1E$	MRCI	21729	0.71	α	0	0	β
	MRCI+Q	19764	−0.71	β	0	0	α
$\tilde{c}^3E$	MRCI	33193	0.96	0	α	α	0
	MRCI+Q	32928					
$\tilde{C}^1A_1$	MRCI	37457	0.77	0	2	0	0
	MRCI+Q	35477	−0.42	0	0	2	0
			−0.42	0	0	0	2
$\tilde{d}^3A_2$	MRCI	37351	1.00	0	0	α	α
	MRCI+Q	37476					
$\tilde{D}^1E$	MRCI	38721	−0.45	0	0	α	β
	MRCI+Q	37492	0.45	0	0	β	α
			−0.54	0	α	0	β
			0.54	0	β	0	α
$\tilde{E}^1E$	MRCI	41279	0.54	0	0	2	0
			−0.54	0	0	0	2
			−0.45	0	α	β	0
	MRCI+Q	40000	0.45	0	β	α	0

[a]Coeff is the coefficient of each determinant, and α, β occupations correspond to spin-up or spin-down electrons. Contours of the relative orbitals are plotted in Figure 1.

ligands (see section III.1), and they polarize the 2s orbital at the "back" of beryllium. The approach of two $Be(NH_3)$ molecules results in a stronger Be−Be bond compared to Be_2. Specifically, the binding energy becomes 22.4, 25.2, and 25.8 kcal/mol at MRCI, MRCI+Q, and CCSD(T), an order of magnitude larger than plain Be_2 values of 1.96, 2.15, and 1.35 kcal/mol. The optimal geometry of $[Be(NH_3)]_2$ has a N−Be−Be−N zigzag skeleton to provide the necessary space for the two beryllium electron pairs and accommodate the same bonding observed for Be_2. The main configuration of the ground state points to the first two resonance structures of Scheme 1 and the next dominant configuration to the last configuration of the same scheme (see Table 4 as well as Figures 4 and 5). The relative contribution of the two configurations does not change significantly going from Be_2 to $[Be(NH_3)]_2$ (coefficients = 0.89 vs 0.89 and −0.26 vs −0.36). This traces back to the small difference between the excitation energy of the $2s^12p^1$-like states of the two systems (^3P and $\tilde{b}^3A_1$), which generate the second configuration: 21978−21981 cm^{-1} ($^3P_{0-2}$)[38] and 21284 cm^{-1} (Table 1). The enhanced binding is rather attributed to the more diffuse nature of the polarized $2s_{Be}$ orbitals in the case of $Be(NH_3)$. Our CCSD(T)/aug-cc-pVTZ polarizabilities for Be and $Be(NH_3)$ are 5.63 and 14.3 $Å^3$. The former compares favorably with the experimental value of 5.60 $Å^3$.[38]

The first three excited electronic states of $[Be(NH_3)]_2$ resemble those of Be_2. The first one ($\tilde{a}^3$ B_g) has a $6a_g^26b_u^12a_u^1$ configuration which is the analogue of one of the $2^3\Pi_g$

Table 4. Vertical Excitation Energy ΔE (cm^{-1}) and Dominant Electronic Configurations for the Lowest Electronic States of $[Be(NH_3)]_2$

			electronic configuration[a]					
state	method	ΔE	coeff	$6a_g$	$7a_g$	$2a_u$	$6b_u$	$2b_g$
$\tilde{X}^1A_g$	MRCI	0	0.89	2	0	0	2	0
	MRCI+Q	0	−0.36	2	2	0	0	0
$\tilde{a}^3B_g$	MRCI	1584	0.94	2	0	α	α	0
	MRCI+Q	1770						
$\tilde{b}^3B_u$	MRCI	4670	0.96	2	α	0	α	0
	MRCI+Q	4665						
$\tilde{A}^1B_g$	MRCI	6381	0.65	2	0	β	α	0
	MRCI+Q	5955	−0.65	2	0	α	β	0
$\tilde{c}^3A_u$	MRCI	12785	0.96	2	α	α	0	0
	MRCI+Q	12838						
$\tilde{B}^1A_u$	MRCI	12861	0.56	2	α	β	0	0
	MRCI+Q	12950	−0.56	2	β	α	0	0
$\tilde{C}^1A_g$	MRCI	13513	0.89	2	0	2	0	0
	MRCI+Q	13180						
$\tilde{d}^3A_g$	MRCI	15647	0.95	2	α	α	0	0
	MRCI+Q	14643						

[a]Coeff is the coefficient of each determinant, and α, β occupations correspond to spin-up or spin-down electrons. Contours of the relative orbitals are plotted in Figure 5.

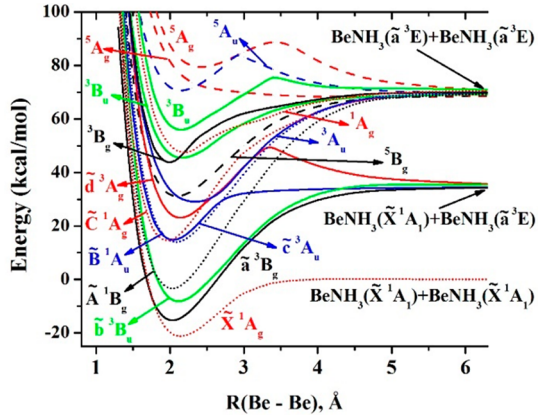

Figure 4. MRCI PEPs of $[Be(NH_3)]_2$ as a function of the Be−Be distance. All other bond lengths and angles are kept fixed to their optimal values of the ground state global minimum.

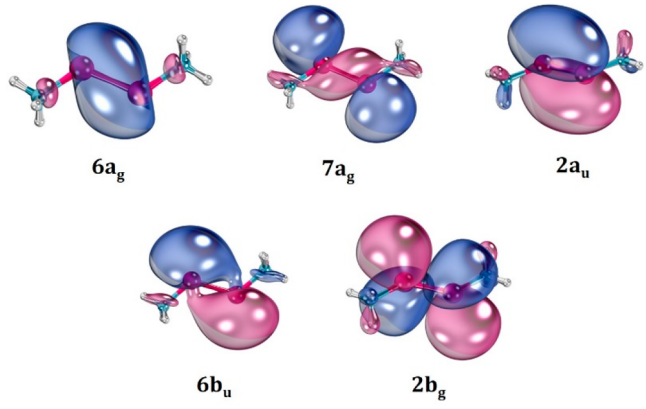

Figure 5. Selected active molecular orbitals of $[Be(NH_3)]_2$.

$(1\sigma_g^21\sigma_u^11\pi_u^1)$ components of Be_2 ($6a_g{\sim}1\sigma_g$; $6b_u{\sim}1\sigma_u$; $2a_u{\sim}1\pi_u$).[8] The symmetry lowering of $[Be(NH_3)]_2$ results to

https://dx.doi.org/10.1021/acs.jpca.0c07939
J. Phys. Chem. A 2020, 124, 9783−9792

the destabilization of one $1\pi_u$ orbital and the shift of the other $2^3\Pi_g$ component to higher energies. The $\tilde{A}^1B_g$ and $3^1\Pi_g$ are the singlet spin counterparts of the two systems, and the $\tilde{b}^3B_u$ corresponds to $1^3\Sigma_u^+$ of Be_2: $6a_g^{\ 2}7a_g^{\ 1}6b_u^{\ 1}$ vs $1\sigma_g^{\ 2}2\sigma_g^{\ 1}1\sigma_u^{\ 1}$ ($7a_g \sim 2\sigma_g$).[8] The excitation energies ΔE are about half or smaller in the $[Be(NH_3)]_2$ case at the MRCI level of theory: $\Delta E(\tilde{a}^3B_g/2^3\Pi_g)$ = 1584/8604 cm^{-1}, $\Delta E(\tilde{A}^1B_g/3^1\Pi_g)$ = 4670/14007 cm^{-1}, and $\Delta E(\tilde{b}^3B_u/1^3\Sigma_u^+)$ = 6381/7508 cm^{-1}.[8]

The addition of a second ammonia ligand to the system polarizes further $2s_{Be}$. The CCSD(T)/aug-cc-pVTZ polarizability becomes 39.7 Å^3. As a result, the Be−Be binding energy for two $Be(NH_3)_2$ systems is larger by about 4 kcal/mol at all three levels of theory: 26.6 [MRCI], 29.4 [MRCI+Q], and 29.4 kcal/mol [CCSD(T)]. The coefficients for the two electronic configurations are 0.91 and −0.34, and the x−Be−Be−x line keeps the zigzag character (x = middle point between two N atoms of the same Be center) to accommodate the same binding scheme. Note also that although CCSD(T) fails considerably for Be_2 (see section III.1), it performs very well when ammonia ligands are present; compare the MRCI +Q and CCSD(T) values of this section. This observation confirms the difficulty to obtain accurate energetics for small quantities such as the binding energy of purely weak molecular interactions.

The case of $[Be(NH_3)_3]_2$ differs significantly. The two additional ammonias in the system force the displacement of a $2s_{Be}$ electron pair to the periphery of a $[Be(NH_3)_3]_2^{2+}$ core, as happens going from $Be(NH_3)_3$ to $Be(NH_3)_4$. A covalent bond forms between two $(NH_3)_3Be^{\bullet+}$ radicals, and the excessive repulsion due to two positively charged molecules is balanced out by the attraction of the $[Be(NH_3)_3]_2^{2+}$ core and the two outer electrons. The absence of the two outer electrons causes the destabilization of the system reducing the dissociation energy to two $(NH_3)_3Be^+$ fragments (see also section III.4). The Be−Be binding energy at MP2 is 35.0 kcal/mol. Because MRCI or CCSD(T) calculations were impractical, we resorted to MP2 calculations. For a fair comparison, the MP2 binding energies for the smaller systems Be_2, $[Be(NH_3)]_2$ and $[Be(NH_3)_2]_2$ are 1.05, 28.3, and 37.2 kcal/mol, meaning that the Be−Be bond for $[Be(NH_3)_3]_2$ drops slightly compared to $[Be(NH_3)_2]_2$.

The trends for the Be−Be bond lengths agree with these of the binding/interaction energies. The bonds for Be_2, $[Be(NH_3)]_2$, $[Be(NH_3)_2]_2$, and $[Be(NH_3)_3]_2$ are 2.477, 2.125, 2.071, and 2.178 Å long. The Be−Be bond contracts considerably in the presence of ammonia ligands despite the increased steric repulsions. The bond shortening is larger for $[Be(NH_3)_2]_2$ which also has the larger binding energy.

A completely different picture from any of the previous systems is found when two more ammonia ligands are included in the system. There is no direct Be−Be bond anymore, but instead two $Be(NH_3)_4$ moieties attach to each other as in Be_2. Be and $Be(NH_3)_4$ have similar electronic structures in the sense that their ground and first excited states have s^2 and s^1p^1 character. In the former case s and p correspond to the $2s_{Be}$ and $2p_{Be}$ atomic orbitals but in the latter to diffuse "superatomic" orbitals of the $Be(NH_3)_4^{2+}$ complex.[21] The excitation energy in the two systems is 2.725 and 0.81 eV,[16,21] suggesting that the contribution of the second Lewis structure of Scheme 1 will contribute more to the wave function of the ground state $[Be(NH_3)_4]_2$ molecule. The coefficients for the relative two configurations are in agreement showing a smaller ratio between the first two coefficients of the CI vector: c_1 = 0.82 and c_2 = −0.34 (c_1/c_2 = 2.4 or c_1^2/c_2^2 = 5.8) vs c_1 = 0.89 and c_2= −0.26 (c_1/c_2 = 3.4 or c_1^2/c_2^2 = 11.7) for Be_2.

The MP2 $(NH_3)_4Be-Be(NH_3)_4$ binding energy is 3 times larger (7.26 kcal/mol or 2539 cm^{-1}) than plain Be−Be. The larger binding energy can be ascribed to two factors: the larger contribution of its first excited state in the bonding and the higher polarizability of $Be(NH_3)_4$. At the MP2/aug-cc-pVTZ level of theory, the two polarizabilities are 6.31 and 71.7 Å^3. The CASPT2 binding energy in the case of the clear covalent $(NH_3)_4Li-Li(NH_3)_4$ and $(NH_3)_4Na-Na(NH_3)_4$ bonds is 14.7 and 5.6 kcal/mol, respectively.[25] Both saturated sodium and lithium ammonia solutions form bronze liquid metal materials.[40,41] Based on the comparable $(NH_3)_4Be-Be(NH_3)_4$ binding energy, the formation of beryllium ammonia liquid metals is possible.

The PEPs for the five lowest energy states of $[Be(NH_3)_4]_2$ as a function of the Be−Be distance are plotted in Figure 6;

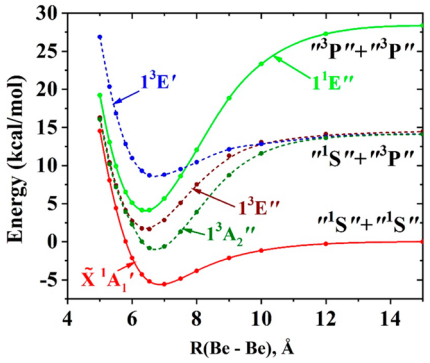

Figure 6. CASPT2 PEPs of $[Be(NH_3)_4]_2$ as a function of the Be−Be distance. All other bond lengths and angles are kept fixed to their DFT/B3LYP optimal values of the ground state at each Be−Be distance. The states of the $Be(NH_3)_4$ fragments are denoted by using the corresponding atomic terms of atomic Be: $^1S(1s^22s^1)$ and $^{1,3}P(1s^22p^1)$.

vertical excitation energies at the CASSCF and CASPT2 levels are tabulated in Table 5 along with the dominant electronic configurations (see Figure 7 for the involved molecular orbitals). The PEPs and electronic configurations echo those of Be_2 reflecting the similarity between Be and $Be(NH_3)_4$. Specifically, the first four states of $[Be(NH_3)_4]_2$ are $\tilde{X}\ ^1A_1'$,

Table 5. CASSCF and CASPT2 Vertical Excitation Energy ΔE (cm^{-1}) and Dominant Electronic Configurations for the Lowest Electronic States of $[Be(NH_4)]_2$

	ΔE			configuration[a]				
state	CASSCF	CASPT2	coeff	$1a_1'$	$2a_1'$	$1a_2''$	$1e_x'$	$1e_y'$
$\tilde{X}^1A_1'$	0	0	0.82	2	0	2	0	0
			−0.34	2	2	0	0	0
$1^3A_2''$	1564	1557	0.92	2	α	α	0	0
$1^3E''$[b]	2567	2579	0.85	2	0	α	α	0
$1^1E''$[b]	3679	3537	0.59	2	0	α	0	β
			−0.59	2	0	β	0	α
$1^3E'$[b]	4693	4772	0.68	α	0	2	α	0
			0.43	2	α	0	α	0

[a]Coeff is the coefficient of each Slater determinant, and α, β occupations correspond to spin-up or spin-down electrons. Contours of the relative orbitals are plotted in Figure 7. [b]The electronic configuration of one out of the two degenerate components is listed.

https://dx.doi.org/10.1021/acs.jpca.0c07939
J. Phys. Chem. A 2020, 124, 9783−9792

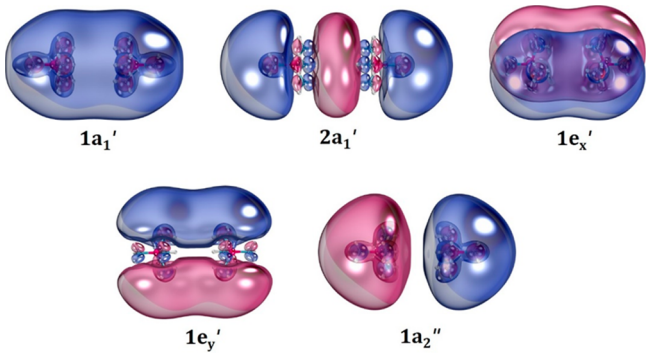

Figure 7. Selected active molecular orbitals of $[Be(NH_3)_4]_2$. Only outer orbitals are counted.

$1^3A_2''$, $1^3E''$, and $1^1E''$, which have identical energy order and electronic structure to the first four states ($X^1\Sigma_g^+$, $1^3\Sigma_u^+$, $2^3\Pi_g$, and $3^1\Pi_g$) of Be_2; compare configurations of Table 5 and those of Be_2 in ref 8. The excitation energies of $[Be(NH_3)_4]_2$ are at least 3 times smaller because of the diffuse nature of its molecular orbitals (see Table 5 and Table 2 of ref 8). The $[Be(NH_3)_4]_2$ and Be_2 PEPs for these states have similar morphology and dissociate to the same states of the fragments (compare present Figure 6 and Figure 6 of ref 8). A noticeable difference is that the ground state PEP is steeper and more bound for $[Be(NH_3)_4]_2$. The fifth state of $[Be(NH_3)_4]_2$ ($1^3E'$) is also bound and dissociates to the "^1S" and "^3P" fragments (analogue ^1S and ^3P states of Be). On the other hand, the corresponding $5^3\Pi_u$ of Be_2 is purely repulsive. Finally, we observe that excitation energies at the CASSCF and CASPT2 levels differ by less than 200 cm^{-1} (see Table 5) due to the partial inclusion of the dynamic electron correlation (see section III.2).

III.4. Cationic Species $Be(NH_3)_{0-4}^+$ and Their Dimers.

The removal of one electron from Be creates the radical $Be^+(^2S; 1s^22s^1)$ species. Ammonia molecules bind easier now to Be^+ guided by the positive charge and the presence of only one electron in 2s, which screens less efficiently the Be^{2+} nuclear charge. As a result, the PECs with respect to the addition of one ammonia are all highly attractive (see Figure S2) leading to $(NH_3)_{n-1}Be^+-NH_3$ CCSD(T) binding energies of 78.3, 51.1, and 38.3 kcal/mol for n = 1, 2, and 3, respectively. The corresponding Be−N bond lengths are 1.681, 1.724, and 1.765 Å. Both the decreasing trend of binding energies and increasing trend of bond lengths are due to the steric repulsion among the ammonia molecules.

Two Be^+ cations repel each other, but they can also bind via a covalent bond. Similar electronic structure and identical interactions occur for two $Be(NH_3)_{n=1-4}^+$ species. Interestingly, the first and last members of the series (Be^+ and $Be(NH_3)_4^+$) create metastable or unstable dimers. There is a Be_2^{2+} minimum, but it is nearly 50 kcal/mol higher than the $Be^+ + Be^+$ fragments at MRCI, in agreement with the CCSD(T) value of ref 14. In addition, we were not able to capture a stable $[Be(NH_3)_4]_2^{2+}$ minimum. However, the covalent bond counterbalances the Coulombic repulsion for the $Be(NH_3)_{1,2,3}^+$ dimers, which have lower energy than the corresponding fragments by 16.2/11.2, 22.9/18.3, and NA/7.13 kcal/mol (NA = not available) at the CCSD(T)/MP2 levels (using the aug-cc-pVTZ basis set), respectively. For comparison, the binding energy of the dimer of the isovalent neutral $(CO)_3Li^\bullet$ radical is 4 times larger (27.2 kcal/mol).[42]

Notice that the MP2 binding energies are smaller by 4−5 kcal/mol for $[Be(NH_3)_{1,2}]_2^{2+}$, and thus the CCSD(T) binding energy for $[Be(NH_3)_3]_2^{2+}$ is expected to be around 12 kcal/mol. In any case, it is the less stable among these species, maybe because of the enhanced repulsion between ammonia ligands of different beryllium centers. Interestingly, the $(NH_3)_3Be-Be(NH_3)_3$ bond gets significantly stronger when two electrons are added to the system (see section III.3). Similar dicationic (RuO^{2+}, MoO^{2+}, and TM_2^{2+}, TM = transition metal)[43−45] or dianionic ($((B_{12}I_9)_2^{2-}$)[46] systems have been observed in the past.

The optimal structures for the stable cationic dimers differ from the corresponding neutral dimers. The N−Be−Be−N and x−Be−Be−x (see section III.3 for definition of x) lines are now collinear because of the absence of electrons in the $2s_{Be}-2s_{Be}$ antibonding orbital. The $[Be(NH_3)_{1,2,3}]_2^{2+}$ structures resemble those of ethyne, ethene, and ethane molecules. The Be−Be bond length increases respectively with the number of ammonia ligands as 2.086, 2.170, and 2.326 Å, while the Be−N bond lengths change within 0.05 Å during the dimerization. Finally, it should be stated that the wave function for all cationic or dicationic systems is pure single-reference with the main coefficient of the CI expansion being 0.95 or higher.

The PEPs for the ground state of $Be(NH_3)_{1,2}^+$ dimers are shown in Figure 7. As expected, they are repulsive for long Be−

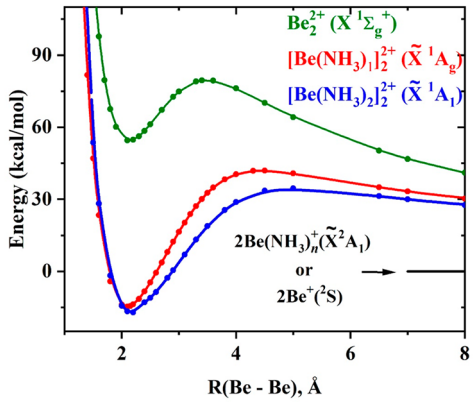

Figure 8. MRCI PEPs of $[Be(NH_3)_{0,1,2}]_2^{2+}$ as a function of the Be−Be distance. All other bond lengths and angles are kept fixed to their optimal values of the ground state global minimum.

Be distances. After an energy barrier at 4.5 and 5.0 Å of 42 and 35 kcal/mol, they turn attractive, forming the equilibrium dimer structures. We were not able to make the PECs for $Be(NH_3)_3^+$, but based on the trends for $Be(NH_3)_{1,2}^+$, we expect a smaller activation barrier occurring at longer distances: The more and more diffuse nature of the unpaired electron going from $Be(NH_3)^+$ to $Be(NH_3)_3^+$ enables the formation of the chemical bond "faster".

IV. CONCLUSIONS

High-level electronic structure methodologies are applied to study the Be−Be bond in the naked Be_2 and when it is coordinated with ammonia ligands. To this end, the electronic structure of the $Be(NH_3)_{n=0-4}$ units was investigated first. We found that ammonia, as opposed to other ligands, retains the ground state $1s^22s^2$ character of Be by polarizing the 2s orbital away from ammonia molecules. We propose for the first time that the bonding between two such closed-shell units can be

https://dx.doi.org/10.1021/acs.jpca.0c07939
J. Phys. Chem. A 2020, 124, 9783−9792

described as a give-and-take mechanism of an electron pair of each $Be(NH_3)_{n=0-4}$ monomer. This picture is rationalized in terms of the Lewis acidity and basicity of beryllium: closed-shell beryllium centers as opposed to rage gas atoms can equally donate an electron pair and polarize to accept an electron pair. This bonding scheme explains the weak, but not so weak, bond in Be_2. The higher polarizability of the ligated units can explain the significantly larger binding energy of their dimers. The previously proposed double bond between two excited ^3P Be atoms is presently found to have small contribution to the formation of the ground state of Be_2 and $(NH_3)_{n=1-3}Be-Be(NH_3)_{n=1-3}$ bonds.

Our larger beryllium ammonia coordination complex, $Be(NH_3)_4$, has two diffuse electrons around a $Be(NH_3)_4^{2+}$ core and imitates the electronic structure of Be. Two such units also bond together as happens for Be_2, and their binding energy is also (3−4 times) larger than that of Be_2. The low-lying excited states for the two dimers have identical electronic configurations and PEPs with similar morphology. However, the excitation energies of both the monomers and dimers are significantly lower in the case of beryllium−ammonia complexes.

The present work and previous literature indicate that there are two ways to enhance the Be−Be bond. The first way is by promoting the Be center to an excited state as happens for H, F, and CO and has been described in the literature (see the Introduction). The second way is by rendering the $2s^2$ electrons of beryllium more polarizable by adding NH_3 ligands or probably other ligands with lone electron pairs such as water or alcohols.

The cationic $Be(NH_3)_{0-4}^+$ species and their dimers were also investigated. In these systems, the repulsion between two positively charged units deters the formation of a single covalent bond. It turns out that Be^+ creates a metastable dimer, $Be(NH_3)_4^+$ does not form a stable dimer, but the intermediate complexes $Be(NH_3)_{1,2,3}^+$ do form dimers with energies lowest than the dissociation limit and protected by large dissociation barriers.

Potential energy profiles for the ground and excited electronic states have been plotted for the monomers and dimers. We believe that our calculated optimized geometries, harmonic vibrational frequencies, binding energies for the ground states, and excitation energies for several low-lying excited electronic states for these exotic molecular systems will allow the experimental identification and characterization of these species in the future. Beryllium−ammonia liquid metals are finally predicted as novel materials by our calculations.

■ ASSOCIATED CONTENT

Supporting Information

The Supporting Information is available free of charge at https://pubs.acs.org/doi/10.1021/acs.jpca.0c07939.

Additional plots of potential energy profiles; tables with optimized geometries and harmonic vibrational frequencies (PDF)

■ AUTHOR INFORMATION

Corresponding Author

Evangelos Miliordos − *Department of Chemistry and Biochemistry, Auburn University, Auburn, Alabama 36849, United States;* orcid.org/0000-0003-3471-7133; Email: emiliord@auburn.edu

Author

Isuru R. Ariyarathna − *Department of Chemistry and Biochemistry, Auburn University, Auburn, Alabama 36849, United States;* orcid.org/0000-0002-5259-4248

Complete contact information is available at: https://pubs.acs.org/10.1021/acs.jpca.0c07939

Notes

The authors declare no competing financial interest.

■ ACKNOWLEDGMENTS

The authors are indebted to Auburn University (AU) for financial support. This work was completed with resources provided by the Auburn University Hopper Cluster and Alabama Supercomputer Center. This material is based upon work supported by the National Science Foundation under Grant CHE-1940456. Any opinions, findings, and conclusions or recommendations expressed in this material are those of the author(s) and do not necessarily reflect the views of the National Science Foundation.

■ REFERENCES

(1) Huber, K. P.; Herzberg, G. *Molecular Spectra and Molecular Structure*; Springer: Boston, MA, 1979.

(2) Wüest, A.; Merkt, F. Determination of the Interaction Potential of the Ground Electronic State of Ne_2 by High-Resolution Vacuum Ultraviolet Laser Spectroscopy. *J. Chem. Phys.* **2003**, *118* (19), 8807−8812.

(3) Herman, P. R.; LaRocque, P. E.; Stoicheff, B. P. Vacuum Ultraviolet Laser Spectroscopy. V. Rovibronic Spectra of Ar_2 and Constants of the Ground and Excited States. *J. Chem. Phys.* **1988**, *89* (8), 4535−4549.

(4) Ginter, M. L.; Battino, R. Potential-Energy Curves for the He_2 Molecule. *J. Chem. Phys.* **1970**, *52* (9), 4469−4474.

(5) Focsa, C.; Bernath, P. F.; Colin, R. The Low-Lying States of He_2. *J. Mol. Spectrosc.* **1998**, *191* (1), 209−214.

(6) Merritt, J. M.; Bondybey, V. E.; Heaven, M. C. Beryllium Dimer–Caught in the Act of Bonding. *Science* **2009**, *324* (5934), 1548−1551.

(7) Tong, X.-F.; Yang, C.-L.; Xiao, J.; Wang, M.-S.; Ma, X.-G. Theoretical Study on the Complexes of He, Ne and Ar. *Chin. Phys. B* **2010**, *19* (12), 123102.

(8) Kalemos, A. The Nature of the Chemical Bond in Be_2^+, Be_2, Be_2^-, and Be3. *J. Chem. Phys.* **2016**, *145* (21), 214302.

(9) Montero-Campillo, M. M.; Mó, O.; Yáñez, M.; Alkorta, I.; Elguero, J. The Beryllium Bond. *Adv. Inorg. Chem.* **2019**, *73*, 73−121.

(10) Patkowski, K.; Podeszwa, R.; Szalewicz, K. Interactions in Diatomic Dimers Involving Closed-Shell Metals. *J. Phys. Chem. A* **2007**, *111* (49), 12822−12838.

(11) Sunil, K. K. The Nature of Bonding and Stability of Beryllium Carbonyl $(CO)_2Be-Be(CO)_2$: A Molecule with a Beryllium-Beryllium Double Bond. *J. Am. Chem. Soc.* **1992**, *114* (10), 3985−3986.

(12) Tague, T. J.; Andrews, L. Reactions of Beryllium Atoms with Hydrogen. Matrix Infrared Spectra of Novel Product Molecules. *J. Am. Chem. Soc.* **1993**, *115* (25), 12111−12116.

(13) Narendrapurapu, B. S.; Bowman, M. C.; Xie, Y.; Schaefer, H. F.; Tkachenko, N. V.; Boldyrev, A. I.; Li, G. Dibridged, Monobridged, Vinylidene-Like, and Linear Structures for the Alkaline Earth Dihydrides Be_2H_2, Mg_2H_2, Ca_2H_2, Sr_2H_2, and Ba_2H_2. Proposals for Observations. *Inorg. Chem.* **2020**, *59* (15), 10404−10408.

(14) Cui, Z.; Yang, W.; Zhao, L.; Ding, Y.; Frenking, G. Unusually Short Be-Be Distances with and without a Bond in Be 2 F 2 and in the Molecular Discuses Be_2B_8 and $Be_2B_7^-$. *Angew. Chem., Int. Ed.* **2016**, *55* (27), 7841−7846.

(15) Lundell, K. A.; Olson, J. K.; Boldyrev, A. I. Exploring the Limits of Electronic Transmutation: Ab Initio Study of Li_nBe_n (n = 3−5). *Chem. Phys. Lett.* **2020**, *739*, 136994.
(16) Kramida, A.; Ralchenko, Y.; Reader, J.; NIST ASD Team. *NIST Atomic Spectra Database* (version 5.4); National Institute of Standards and Technology: Gaithersburg, MD, 2016; http://physics.nist.gov/asd (accessed Dec 13, 2019).
(17) Ariyarathna, I. R.; Miliordos, E. The Versatile Personality of Beryllium: $Be(O_2)_{1-2}$ vs $Be(CO)_{1-2}$. *J. Phys. Chem. A* **2017**, *121* (37), 7051−7058.
(18) Kalemos, A.; Ariyarathna, I. R.; Khan, S. N.; Miliordos, E.; Mavridis, A. "Hypervalency" and the Chemical Bond. *Comput. Theor. Chem.* **2019**, *1153*, 65−74.
(19) Ariyarathna, I. R.; Miliordos, E. Electronic and Geometric Structure Analysis of Neutral and Anionic Metal Nitric Chalcogens: The Case of MNX Series (M = Li, Na, Be and X = O, S, Se, Te). *J. Comput. Chem.* **2019**, *40* (19), 1740−1751.
(20) Ariyarathna, I. R.; Miliordos, E. Dative Bonds versus Electron Solvation in Tri-Coordinated Beryllium Complexes: $Be(CX)_3$ [X = O, S, Se, Te, Po] and $Be(PH_3)_3$ versus $Be(NH_3)_3$. *Int. J. Quantum Chem.* **2018**, *118* (18), No. e25673.
(21) Ariyarathna, I. R.; Khan, S. N.; Pawłowski, F.; Ortiz, J. V.; Miliordos, E. Aufbau Rules for Solvated Electron Precursors: $Be(NH_3)_4^{0,\pm}$ Complexes and Beyond. *J. Phys. Chem. Lett.* **2018**, *9* (1), 84−88.
(22) Ariyarathna, I. R.; Miliordos, E. Superatomic Nature of Alkaline Earth Metal−Water Complexes: The Cases of $Be(H_2O)_4^{0,+}$ and $Mg(H_2O)_6^{0,+}$. *Phys. Chem. Chem. Phys.* **2019**, *21* (28), 15861−15870.
(23) Ariyarathna, I. R.; Almeida, N. M. S.; Miliordos, E. Stability and Electronic Features of Calcium Hexa-, Hepta-, and Octa-Coordinated Ammonia Complexes: A First-Principles Study. *J. Phys. Chem. A* **2019**, *123* (31), 6744−6750.
(24) Ariyarathna, I. R.; Pawłowski, F.; Ortiz, J. V.; Miliordos, E. Aufbau Principle for Diffuse Electrons of Double-Shell Metal Ammonia Complexes: The Case of $M(NH_3)_4@12NH_3$, M = Li, Be^+, B^{2+}. *J. Phys. Chem. A* **2020**, *124* (3), 505−512.
(25) Ariyarathna, I. R.; Pawłowski, F.; Ortiz, J. V.; Miliordos, E. Molecules Mimicking Atoms: Monomers and Dimers of Alkali Metal Solvated Electron Precursors. *Phys. Chem. Chem. Phys.* **2018**, *20* (37), 24186−24191.
(26) Ariyarathna, I. R.; Miliordos, E. Geometric and Electronic Structure Analysis of Calcium Water Complexes with One and Two Solvation Shells. *Phys. Chem. Chem. Phys.* **2020**, DOI: 10.1039/D0CP04309E.
(27) Zurek, E.; Edwards, P. P.; Hoffmann, R. A Molecular Perspective on Lithium-Ammonia Solutions. *Angew. Chem., Int. Ed.* **2009**, *48* (44), 8198−8232.
(28) Seel, A. G.; Zurek, E.; Ramirez-Cuesta, A. J.; Ryan, K. R.; Lodge, M. T. J.; Edwards, P. P. Low Energy Structural Dynamics and Constrained Libration of $Li(NH_3)_4$, the Lowest Melting Point Metal. *Chem. Commun.* **2014**, *50* (74), 10778−10781.
(29) Raghavachari, K.; Trucks, G. W.; Pople, J. A.; Head-Gordon, M. A Fifth-Order Perturbation Comparison of Electron Correlation Theories. *Chem. Phys. Lett.* **1989**, *157* (6), 479−483.
(30) Kendall, R. A.; Dunning, T. H.; Harrison, R. J. Electron Affinities of the First-row Atoms Revisited. Systematic Basis Sets and Wave Functions. *J. Chem. Phys.* **1992**, *96* (9), 6796−6806.
(31) Prascher, B. P.; Woon, D. E.; Peterson, K. A.; Dunning, T. H.; Wilson, A. K. Gaussian Basis Sets for Use in Correlated Molecular Calculations. VII. Valence, Core-Valence, and Scalar Relativistic Basis Sets for Li, Be, Na, and Mg. *Theor. Chem. Acc.* **2011**, *128* (1), 69−82.
(32) Shamasundar, K. R.; Knizia, G.; Werner, H.-J. A New Internally Contracted Multi-Reference Configuration Interaction Method. *J. Chem. Phys.* **2011**, *135* (5), 054101.
(33) Knowles, P. J.; Werner, H.-J. An Efficient Method for the Evaluation of Coupling Coefficients in Configuration Interaction Calculations. *Chem. Phys. Lett.* **1988**, *145* (6), 514−522.
(34) Werner, H.; Knowles, P. J. An Efficient Internally Contracted Multiconfiguration−Reference Configuration Interaction Method. *J. Chem. Phys.* **1988**, *89* (9), 5803−5814.
(35) Langhoff, S. R.; Davidson, E. R. Configuration Interaction Calculations on the Nitrogen Molecule. *Int. J. Quantum Chem.* **1974**, *8* (1), 61−72.
(36) Frisch, M. J.; Trucks, G. W.; Schlegel, H. B.; Scuseria, G. E.; Robb, M. A.; Cheeseman, J. R.; Scalmani, G.; Barone, V.; Petersson, G. A.; Nakatsuji, H.; et al. *Gaussian 16*; Gaussian, Inc.: Wallingford, CT, 2016.
(37) Werner, H.-J.; Knowles, P. J.; Knizia, G.; Manby, F. R.; Schütz, M.; Celani, P.; Györffy, W.; Kats, D.; Korona, T.; Lindh, R.; et al. *Molpro: A General-Purpose Quantum Chemistry Program Package*; MOLPRO: version 2015.1; http://www.molpro.net.
(38) Lide, D. R. *CRC Handbook of Chemistry and Physics*, 93rd ed.; CRC Press: New York, 2012.
(39) Shaik, S.; Danovich, D.; Galbraith, J. M.; Braïda, B.; Wu, W.; Hiberty, P. C. Charge-Shift Bonding: A New and Unique Form of Bonding. *Angew. Chem., Int. Ed.* **2020**, *59* (3), 984−1001.
(40) Zurek, E.; Wen, X.-D.; Hoffmann, R. (Barely) Solid $Li(NH_3)_4$: The Electronics of an Expanded Metal. *J. Am. Chem. Soc.* **2011**, *133* (10), 3535−3547.
(41) Buttersack, T.; Mason, P. E.; McMullen, R. S.; Schewe, H. C.; Martinek, T.; Brezina, K.; Crhan, M.; Gomez, A.; Hein, D.; Wartner, G.; et al. Photoelectron Spectra of Alkali Metal−Ammonia Microjets: From Blue Electrolyte to Bronze Metal. *Science* **2020**, *368* (6495), 1086−1091.
(42) Ariyarathna, I. R.; Miliordos, E. Electronic and Geometric Structure Analysis of Neutral and Anionic Alkali Metal Complexes of the CX Series (X = O, S, Se, Te, Po): The Case of $M(CX)_{n=1-4}$ (M = Li, Na) and Their Dimers. *J. Comput. Chem.* **2019**, *40* (13), 1344−1351.
(43) Almeida, N. M. S.; Ariyarathna, I. R.; Miliordos, E. O−H and C−H Bond Activations of Water and Methane by RuO^{2+} and $(NH_3)RuO^{2+}$: Ground and Excited States. *J. Phys. Chem. A* **2019**, *123* (43), 9336−9344.
(44) Zhao, T.; Zhou, J.; Wang, Q.; Jena, P. Like Charges Attract? *J. Phys. Chem. Lett.* **2016**, *7* (14), 2689−2695.
(45) Ariyarathna, I. R.; Miliordos, E. Ab Initio Investigation of the Ground and Excited States of $MoO^{+,2+,-}$ and Their Catalytic Strength on Water Activation. *Phys. Chem. Chem. Phys.* **2018**, *20* (17), 12278−12287.
(46) Liu, F.; Press, M. R.; Khanna, S. N.; Jena, P. Stability of Doubly Charged Transition-Metal Dimers. *Phys. Rev. Lett.* **1987**, *59* (22), 2562−2565.

https://dx.doi.org/10.1021/acs.jpca.0c07939
J. Phys. Chem. A 2020, 124, 9783−9792